

## The growth of $\text{Sb}_2\text{S}_3$ crystals with bend lattice during amorphous films annealing and condensation

A.G.Bagmut, S.N.Grigorov, V.Yu.Kolosov\*,  
V.M.Kosevich, G.P.Nikolaychuk

National Technical University "Kharkiv Polytechnical Institute",  
21 Frunze St., 61002 Kharkiv, Ukraine  
\*Ural State Economic University,  
62, 8 Marta St., 620026 Ekaterinburg, Russia

Received September 10, 2004

Using the electron microscopy methods the process of crystallization of amorphous  $\text{Sb}_2\text{S}_3$  films was investigated. The amorphous films were prepared by the vacuum condensation ( $10^{-5}$  Torr) on a surface of KCl crystals at a temperature of 20–185°C. The crystallization of amorphous films was initiated by their heating with the electron beam in a column of electron microscope (*in situ* technique). The partial crystallization of  $\text{Sb}_2\text{S}_3$  films occurred also directly during the condensation process when the substrate temperature was in the range of 183–185°C. It was established, that in amorphous  $\text{Sb}_2\text{S}_3$  films the crystals with the bent crystal lattice are formed. The local bend of a lattice makes ~20 degree/microns. At a slow heating of a film by an electron beam it was revealed, that at first in a surface layer of the film a thin crystals with the undistorted lattice was nucleated. The bend of a crystal lattice occurs during the increasing of the  $\text{Sb}_2\text{S}_3$  crystals thickness.

Методами электронной микроскопии исследована кристаллизация аморфных пленок  $\text{Sb}_2\text{S}_3$ . Аморфные пленки конденсировались в вакууме  $10^{-5}$  Торр на поверхности кристаллов KCl при температуре подложки 20–185°C. Кристаллизация аморфных пленок осуществлялась путем их нагрева электронным лучом в колонне электронного микроскопа (методика "*in situ*"). Частичная кристаллизация пленок  $\text{Sb}_2\text{S}_3$  происходила также непосредственно в ходе конденсации при температуре подложки 183–185°C. Установлено, что в аморфных пленках  $\text{Sb}_2\text{S}_3$  образуются кристаллы с изогнутой кристаллической решеткой. Локальный изгиб решетки составляет ~20 град/мкм. При медленном нагреве пленки электронным пучком обнаружено, что сначала в приповерхностном слое пленки возникают тонкие кристаллы с неизогнутой решеткой. Изгиб кристаллической решетки происходит в процессе увеличения толщины кристаллов.

Today it is established that during the amorphous films annealing, if they consist of materials crystallizing by spherulites growth [1–5], dislocation-free crystals with strong regular internal bending of the crystal lattice planes (up to 120° per 1  $\mu\text{m}$ ) are formed. This bending called lattice twisting has the character of elastic rotation lattice distortion in the crystal. It was observed at amorphous films crystallization of sele-

mium, copper selenide and copper telluride,  $\text{Cr}_2\text{O}_3$ ,  $\text{Fe}_2\text{O}_3$  etc. The crystals themselves in this case remain flat. The model for internal bending of lattice for crystal grown in a thin amorphous film is shown in Fig. 1 [6]. The crystals with such lattice bending were called "transrotational crystals" in [3]. In [2] it was shown on the example of selenium, stibium selenide and stibium sulphide amorphous films crystallization that the de-

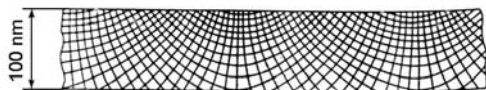


Fig. 1. The model of internal bending in the lattice of crystal, grown in amorphous film [6].

gree of internal bending in crystal lattice with the decrease of amorphous films thickness in the range 100–10 nm increases from 6° to 60° per 1  $\mu\text{m}$ . Nevertheless, the internal bending of the lattice in  $\text{Sb}_2\text{S}_3$  chips on the initial stage of their growth, prior to spherulites formation, was not studied in detail. The aim of our paper is the study on formation of crystals with lattice internal bending in amorphous films of stibium sulphide at different films thickness, condensation temperature and crystal growth velocity.

The crystal phase of stibium sulphide  $\text{Sb}_2\text{S}_3$ , according to JCPDS library data, has orthorhombic lattice with periods  $a = 1.1229$  nm,  $b = 1.1310$  nm and  $c = 0.3839$  nm. Amorphous stibium sulphide films were prepared by thermal vaporization of chemical compound  $\text{Sb}_2\text{S}_3$  in vacuum  $10^{-5}$  Torr. Stibium sulphide powder was vaporized from a molybdenum boat immediately exposed to heavy current. This caused high vaporization rate and low probability of  $\text{Sb}_2\text{S}_3$  molecules dissociation. The condensation took place on the surface of KCl crystal chip (001). The temperature of substrate crystals  $T_S$  changed from room to 200°C. The amorphous films were formed in substrate temperature interval 20–180°C. Polycrystal  $\text{Sb}_2\text{S}_3$  films condensed at  $T_S > 180^\circ\text{C}$ . To settle the start of amorphous  $\text{Sb}_2\text{S}_3$  films crystallization and get amorphous films with imbedded crystals, the substance was condensed on substrate crystals, along which a certain temperature gradient was made. The temperature of "cold" end of the crystal was 180°C. Substrate crystals of room temperature were placed at different distances from the vaporizer, and this made it possible to change the thickness of condensed films stepwise in the interval from 10 to 50 nm. Onto the heated crystals different masses of the substance were condensed, and this also provided films of different thickness.

Local crystallization of separate regions in amorphous films was made *in situ* by heating them with electron beam of various focusing and intensity in electronic microscope PEM-125K column. Crystals several millimeters in size were grown. The growth was stopped for the crystal structure study by reducing the electron beam intensity.

The growth velocity varied in the interval 0.001–1  $\mu\text{m/s}$ .

Structure studies were made by bright and dark field electron microscopy, selected area diffraction and high-resolution electron microscopy methods. The crystals lattice bending was determined basing on the analysis of extinction bend contour patterns, appearing in the image during crystals growth. The peculiarity of these pictures is that they form a stable pattern, depending only on the kind of every chip crystal plate lattice bending. The symmetry of bend contours position and intercontour distances remain almost unchanged in case of exposure and displacing the object under electron beam in the electron microscope, though the centers of band-axis patterns and the contours themselves, of course, move. The integral bend of crystal lattice was defined as the ratio of the angle between the reflecting planes zones axes of adjacent band-axis patterns to the distance between the centers of these patterns. Local lattice bend  $d\varphi/W$  ( $d\varphi$  is the rotation angle of the lattice in the region between the bend extinction contours  $hkl$  and  $h\bar{k}l$ ,  $W$  is the distance between the bend contours) was determined by the methodic [7]:

$$\frac{d\varphi}{W} = \frac{1}{R} = \frac{[1 + (d_{hk0}/d_{00l})^2]\lambda}{Wd_{hk0}},$$

where  $R$  is crystal curvature radius,  $d_{hk0}$  and  $d_{00l}$  are interplane distance of planes ( $hk0$ ) and ( $00l$ ) respectively,  $\lambda$  is the length of de Broglie wave for electrons.

The *in situ* study of amorphous stibium sulphide films crystallization showed that it takes place in two stages. On the first stage, the surplus stibium emerges in the form of many small crystals. The surplus stibium in the film is, evidently, caused by partial decomposition of  $\text{Sb}_2\text{S}_3$  charge, while sulfur, a more volatile component, has vaporized and so the film was exhausted in sulfur. As a result, the composition of the amorphous film tends to the stoichiometric composition of  $\text{Sb}_2\text{S}_3$  compound. The process of stibium emerging ends after the metastable equilibrium in the system is achieved: the amorphous phase of  $\text{Sb}_2\text{S}_3$  – crystal stibium. With further heating of the film the number of stibium crystals and their size don't change.  $\text{Sb}_2\text{S}_3$  crystals form in the amorphous film on the second stage at more intense electron beam. The presence of stibium crystals almost doesn't affect  $\text{Sb}_2\text{S}_3$  crystallization front

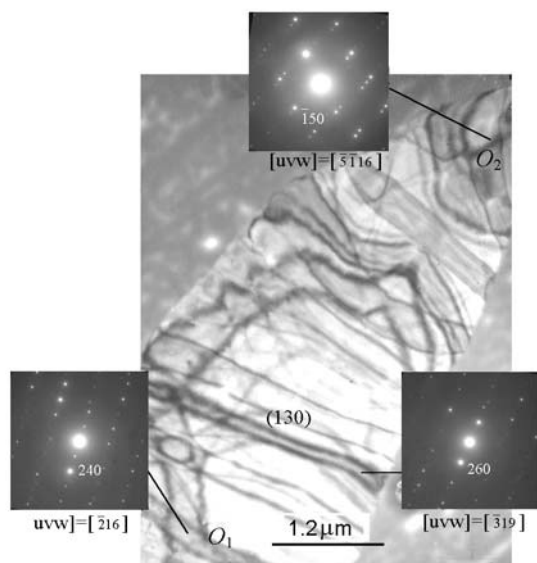


Fig. 2.  $\text{Sb}_2\text{S}_3$  crystal, grown in amorphous film by *in situ* method. The local crystal lattice bend in the region is  $4.2 \text{ grad}/\mu\text{m}$ , where two bending extinction contours of (130) type are situated.

spreading. The moiré patterns on stibium crystals image in the crystallized regions of the film also show that they form on the film surface or in the thin near-surface layer. The same way of crystallization is observed in case of stibium sulphide condensing onto the heated substrate at  $T_S = 180\div 200^\circ\text{C}$ : stibium crystals form at a lower temperature, and  $\text{Sb}_2\text{S}_3$  — at a higher one.

In Fig. 2 electron-microscopy shot of the crystal, grown *in situ* in amorphous stibium sulphide film at high growth velocity ( $\sim 1 \mu\text{m/s}$ ), and selected area diffraction patterns from different its regions are shown. The integral bending of the crystal lattice, estimated in the region between the axes of  $O_1$  and  $O_2$  zones, is  $5.2^\circ$  per  $1 \mu\text{m}$ . The local bending, estimated in the region of two contours (130), is  $4.2^\circ$  per  $1 \mu\text{m}$ , which is in accord with the determined integral bending. The crystals of this type were grown in amorphous films, condensed both at room temperature of substrate and at  $180^\circ\text{C}$ . For various crystals we have observed a local crystal lattice bending about  $8\text{--}15^\circ$  per  $1 \mu\text{m}$ .

In Fig. 3 we can see electron microscopy shot of a crystal with complicated and repeating bend contour pattern. This crystal was grown *in situ* from a needle-shaped crystallizing nucleus, formed in stibium sulphide amorphous film during its condensation at  $T_S = 180^\circ\text{C}$ . In the crystal region

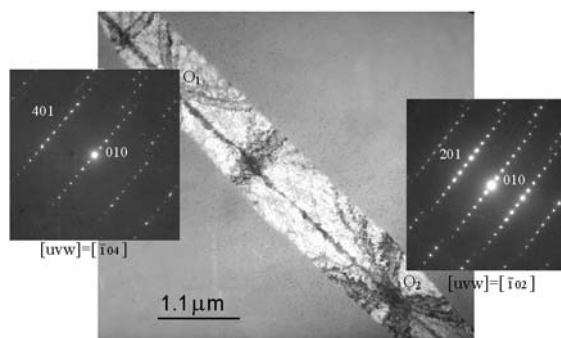


Fig. 3.  $\text{Sb}_2\text{S}_3$  crystal, grown in amorphous film by *in situ* method from a needle-shaped nucleus formed by condensation of the film ( $T_S = 180^\circ\text{C}$ ). The crystal lattice rotation angle between the axes of  $O_1$  and  $O_2$  zones is  $19.5^\circ$ .

$4 \mu\text{m}$  long between the axes of  $O_1$  and  $O_2$  zones, the turn of lattice around the axis, perpendicular to the crystal axis, is  $19.5^\circ$ . A similar pattern of bend extinction contours was observed in the image of  $\text{Cu}_{2-x}\text{Te}$  crystals [4]. It was shown by calculation of simulated bend contour patterns that the electron-microscopic contrast can be obtained in the image of a "transrotational" crystal with an additional bend around its longitudinal axis. The crystal in Fig. 3 may have the same character of lattice distortion.

For this experiment, we have prepared amorphous films, 4–5 times differing in thickness. At stepwise thickness reducing in the amorphous films, we did not observe such an essential increase of lattice curvature of the  $\text{Sb}_2\text{S}_3$  crystals grown in them, as was found in [2] at continuous reducing of films thickness. It was only noticed that the thinner the film is, the higher is the current density at which it crystallizes. Films less than  $10 \text{ nm}$  thick did not crystallize even at maximum current density of the electron beam, achieved in the aperture diaphragm of the second condenser absence. In such films the electron beam caused only explosive crystallization near cracks in the film, resulting in microcrystalline structure forming. Crystallization impediment at film thickness reducing corresponds to a well-known regularity of amorphous state stability increase with the reducing of condensing films thickness [8, 9].

At slow heating of the amorphous film by electron beam and, so, small crystals growth velocity ( $\sim 0.001 \mu\text{m/s}$ ) it was established that at the first stage of crystallization appear very thin crystal wafers with the thickness much smaller than the film thickness. The diffraction contrast in

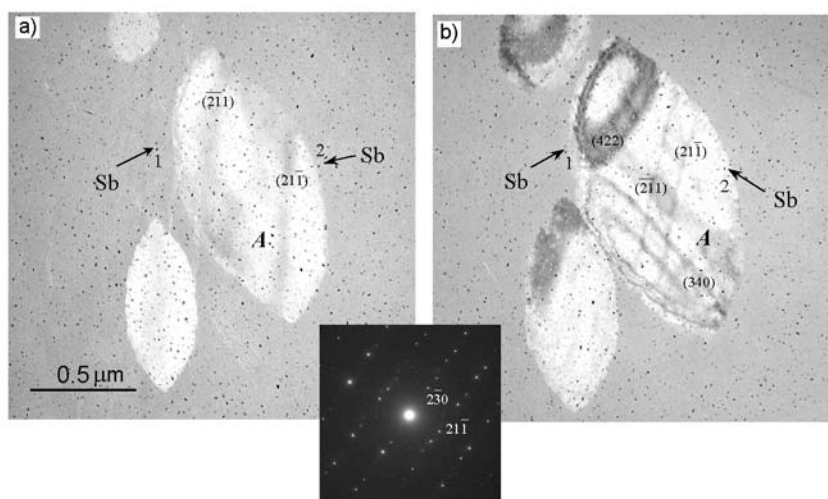


Fig. 4. Crystal lattice bend during the crystal growth in amorphous film: a) the initial stage of crystallization; b) the same region after 5 min exposure to electron beam.

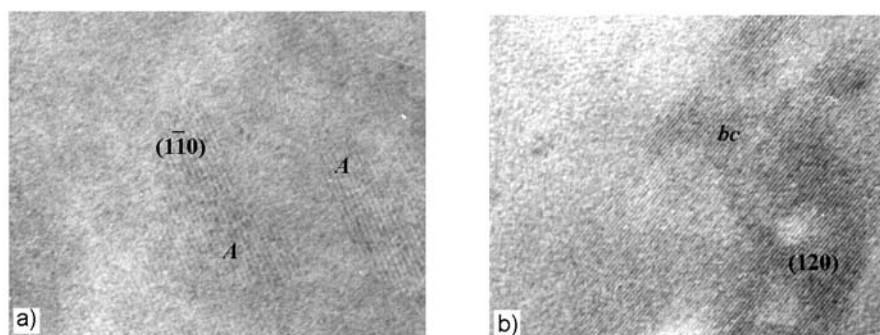


Fig. 5. Crystal lattice bend during the crystal growth in amorphous film. a) thin crystal wafers A with non-bound crystal lattice in the amorphous matrix ( $d_{(110)} = 0.799$  nm); b) the same region after the exposure to cathode beam. In the crystal shot bending extinction pattern bc with planes resolution (120) ( $d_{(120)} = 0.505$  nm) is observed.

their image is very weak, bend extinction contours either are absent or are very wide and mostly only one, but not a couple of contours from like planes, is observed. This implies minor curvature of the crystal lattice. With the further heating the size of the plates in the film plane does not increase much, but they intergrow in all the thickness in the amorphous film. As the thickness of crystal wafers increase, the width of bend extinction contours reduces, pairs of bend contours from the like planes appear, intercontour distance decreases and contours from other plane systems appear. This denotes the curvatures increase in the lattice. For instance, in Fig. 4a,b two electron microscopy shots made with 5 min interval of the same crystals, grown in stibium sulphide amorphous film by slow heating. Fig. 4a shows very thin  $\text{Sb}_2\text{S}_3$  crystals. The local curvature of crystal A lattice, calculated by the distance between the bend contours  $(\bar{2}11)$  and  $(21\bar{1})$ , is  $2.9^\circ$  per  $1 \mu\text{m}$ .

In the shot Fig. 4b the local curvature of the lattice, calculated by intercontour distance between the same pair of bend contours, is  $9.5^\circ$  per  $1 \mu\text{m}$ . The increase of lattice curvature from the center to the periphery in the crystals is noticeable. For example, in crystal A, in the regions where a pair of bend extinction contours (340) is situated, it increases from  $9.5^\circ$  per  $1 \mu\text{m}$  in the central part of the crystal up to  $19^\circ$  per  $1 \mu\text{m}$  near the edge of the crystal. In the amorphous film surrounding the crystals, no morphological changes are observed.

The increase of crystal lattice curvature with crystals thickness increase was also observed in case of *in situ* crystallization in high-resolution electron microscopy mode. Figs. 5a,b show the shots of one and the same film region, taken at different crystallization stages under the influence of electron beam. In Fig. 5a within crystal wafer atomic planes are resolved (110). With crys-

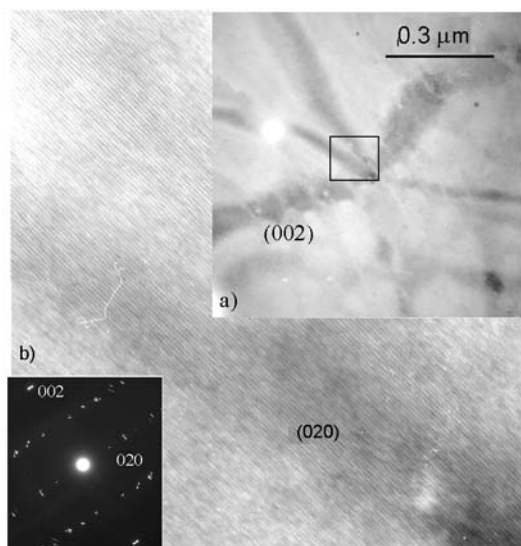


Fig. 6. Amorphous  $\text{Sb}_2\text{S}_3$  film during crystallization: a) the crystal with dome-like lattice. Local crystal lattice bending in the contour region (002) is  $\sim 20$  grad/ $\mu\text{m}$ ; b) the resolution of atomic planes (020) in the region marked in the picture with a rectangle (a) ( $d_{(020)} = 0.566$  nm).

tal region expansion and thickening, the lattice bends. In the wafer image (Fig. 5b) bend extinction contour  $bc$  appears and the system of planes comes to reflecting state (120).

Relative change of  $\text{Sb}_2\text{S}_3$  films density in amorphous and crystal states is evaluated by methodic [5]. To do it, the change of distance between the same Sb crystals (black points 1 and 2 in Fig. 4) near  $\text{Sb}_2\text{S}_3$  crystal for the time of its thickness increase at the exposure to the intensive electron beam was determined. It was found that the relative substance density increase at amorphous  $\text{Sb}_2\text{S}_3$  films crystallization is  $\sim 8\%$ . So, one can expect that the crystals in the film plane are influenced by tension stress. In spite of it, their crystal lattice is curved.

The films condensed at substrate temperature  $183\text{--}185^\circ\text{C}$  were mostly amorphous, but contained ingrained stibium crystals and  $\text{Sb}_2\text{S}_3$  crystals.  $\text{Sb}_2\text{S}_3$  crystals had the typical form for crystals formed at amorphous films crystallization, which essentially differs from the form they have in case of "vapor-crystal" film growth mechanism [10]. This implies that  $\text{Sb}_2\text{S}_3$  crystals appeared as a result of  $\text{Sb}_2\text{S}_3$  amorphous film crystallization. In electron microscopic images of these crystals bend extinction contours, making the pattern, typical for the bend of their lattice, were observed. In

particular, the same patterns of bend contours were observed in [5] in  $\text{Cr}_2\text{O}_3$  crystals. In Fig. 6 electron microscopy shot and selected area diffraction pattern of a crystal with a dome-shaped lattice bending are shown. The resolution of atomic planes (020) is shown in the region, marked in the picture with a rectangle. The local crystal lattice bend, evaluated by intercontour distance of (002) type bend extinction contour is  $\sim 20^\circ$  per  $1\ \mu\text{m}$ . For various crystals with different types of bending the local lattice bend was calculated. It is  $5\text{--}20^\circ$  per  $1\ \mu\text{m}$ . The dependence of bend value on the film thickness is not established.

Thus, it is found out that at  $\text{Sb}_2\text{S}_3$  amorphous films crystallization by heating with a electron beam immediately in the electronic microscope column, as well as in case of crystallization by condensation at substrate temperature  $183\text{--}185^\circ\text{C}$  there appear  $\text{Sb}_2\text{S}_3$  crystals in films with a bound crystal lattice. The local bend of the lattice is  $5\text{--}20^\circ$  per  $1\ \mu\text{m}$ . It is discovered that if the film is slowly heated with a electron beam, then, first in the subsurface regions of the film, thin crystals with non-bound lattice appear. The bend of the crystal lattice takes place with the increase of crystals thickness, when the crystallization front is moving along the normal to the film surface.

The work was done with INTAS financial support (grant No.00-100).

### References

1. I.Ye.Bolotov, V.Yu.Kolosoov, V.B.Malkov, *Kristallografia*, **31**, 204 (1986).
2. V.Yu.Kolosoov, L.M.Veretennikov, *Surface. X-Ray, Synchrotron and Neutron Studies*, No.2, 70 (2000).
3. V.Yu.Kolosoov, A.R.Tholen, *Acta Materialia*, **48**, 1829 (2000).
4. V.Yu.Kolosoov, A.R.Tholen, *Proc. ICEM-15*, **1**, 957 (2002).
5. A.G.Bagmut, S.N.Grigorov, V.Yu.Kolosoov et al., *Functional Materials*, **10**, 687 (2003).
6. V.Yu.Kolosoov, *Proc. of EUREM-92. Granada: Electron Microscopy*, **2**, 513 (1992).
7. I.Ye.Bolotov, V.Yu.Kolosoov, *Izv.AN SSSR, Ser. Phys.*, **44**, 1194 (1980).
8. V.P.Zakharov, V.S.Gerasimenko, *Structure Properties of Semiconductors in Amorphous State*, Kyiv, Naukova Dumka (1976) [in Russian].
9. L.S.Palatnik, V.M.Kosevich, M.Ya.Fuks, *Condensed Films Forming Mechanism and Substructure*, Nauka, Moscow, (1972) [in Russian].
10. V.M.Kosevich, L.F.Zozulya, *Kristallografia*, **26**, 640 (1981).

## **Ріст кристалів $\text{Sb}_2\text{S}_3$ з вигнутою кристалічною решіткою при відпалі аморфних плівок у в процесі конденсації**

**О.Г.Багмут, С.М.Григоров, В.Ю.Колосов,  
В.М.Косевич, Г.П.Ніколайчук**

Методами електронної мікроскопії досліджено кристалізацію аморфних плівок  $\text{Sb}_2\text{S}_3$ . Аморфні плівки сконденсовані у вакуумі  $10^{-5}$  Торр на поверхні кристалів КС1 при температурі підкладки 20–185°C. Кристалізація аморфних плівок здійснювалася шляхом їх нагріву електронним променем у колонні електронного мікроскопа (методика "in situ"). Часткова кристалізація плівок відбувалася також безпосередньо під час конденсації при температурі підкладки 183–185°C. Встановлено, що в аморфних плівках  $\text{Sb}_2\text{S}_3$  виникають кристали з вигнутою кристалічною решіткою. Локальний вигін решітки складає ~20 град/мкм. При повільному нагріві плівки електронним променем знайдено, що спочатку у приповерхньому шарі плівки виникають тонкі кристали з невивгнутою решіткою. Вигін кристалічної решітки відбувається у процесі збільшення товщини кристалів.